# Synthesis, Characterization, and DNA-Binding Properties of the Ruthenium(II) Complexes [Ru(dipn)(dptp)](ClO$_4$)$_2$ and [Ru(dipn)(pat)](ClO$_4$)$_2$ (dipn = *N*-(3-Aminpropyl)propane-1,3-diamine; dptp = 2-(5,6-Diphenyl-1,2,4-triazin-3-yl)-1,10-phenanthroline; pat = 9-(1,10-Phenanthrolin-2-yl)acenaphtho[1,2-*e*][1,2,4]triazine)

by **Xian-Lan Hong**[a][c], **Hui Chao***[a], **Li-Jun Lin**[a], **Kang-Cheng Zheng***[a], **Hong Li**[d], **Xiang-Li Wang**[a], **Feng-Cun Yun**[a], and **Liang-Nian Ji***[a][b]

[a]) Department of Chemistry, Sun Yat-Sen University, Guangzhou 510275, P. R. China (fax: +86-20-84035497; e-mail: ceschh@zsu.edu.cn)

[b]) State Key Laboratory of Gene Engineering of Ministry of Education, Sun Yat-Sen University, Guangzhou 510275, P. R. China

[c]) Department of Chemistry, Shaoguan University, Shaoguan, Guangdong 512005, P. R. China

[d]) Department of Chemistry, Southern China Normal University, Guangzhou 510631, P. R. China

Two novel tridentate ruthenium(II) complexes containing an asymmetric heteroaromatic and a polyamine ligand, [Ru(dipn)(dptp)](ClO$_4$)$_2$ (**1**·2 ClO$_4^-$) and [Ru(dipn)(pat)](ClO$_4$)$_2$ (**2**·2 ClO$_4^-$) (dipn = *N*-(3-aminopropyl)propane-1,3-diamine; dptp = 2-(5,6-diphenyl-1,2,4-triazin-3-yl)-1,10-phenanthroline; and pat = 9-(1,10-phenanthrolin-2-yl)acenaphtho[1,2-*e*][1,2,4]triazine) were synthesized and characterized by elemental analysis, ESI-MS, $^1$H-NMR, UV/VIS, and cyclic voltammetry. The DNA-binding behavior of both complexes was studied by absorption titration, thermal denaturation, and viscosity measurements. Results indicate that complex **2** binds to calf-thymus DNA in an intercalative mode but complex **1** binds to DNA in partial intercalation, and the DNA-binding affinity of complex **2** is much greater than that of complex **1**. Theoretical studies for these complexes were also carried out with the density-functional-theory (DFT) method. The trend in the DNA-binding affinity and some electrochemical and spectral properties of the complexes can be further explained applying the DFT computational results.

**1. Introduction.** – Over the past decade, tremendous interest has been attracted to the interactions of substitution-inert metal complexes with nucleic acids [1–3]. In particular, ruthenium(II) complexes with polypyridine ligands, due to a combination of easily constructed rigid chiral structures spanning all three spatial dimensions and a rich photophysical repertoire, have attracted considerable attention [2–12]. However, the vast majority of these studies have focused on the structural analogues based on the prototype [Ru(bpy)$_3$]$^{2+}$ or [Ru(phen)$_3$]$^{2+}$, where bpy and phen stand for 2,2′-bipyridine and 1,10-phenanthroline, respectively. Investigations of ruthenium(II) complexes with tridentate ligands have received a limited degree of attention [13–15], their exact mode and extent of DNA binding still remain unknown. In fact, molecular shape, among the various factors that contribute to stabilize the metal complex on the DNA helix, appears to be the most significant. Therefore, extensive studies with structurally different tridentate ligands are necessary to evaluate and understand the factors that determine the DNA-binding mode.

On the other hand, although such $Ru^{II}$ complexes have been synthesized and experimentally studied, the theoretical reports on them are relatively scarce. It is very important and necessary to carry out the theoretical studies based on the experimental findings to discuss the interaction mechanism between the complex and DNA and to further guide the molecular design of such types of complexes. At present, various theoretical researches have been carried out in attempts to correlate experimental results to theoretical predictions. In particular, the quantum-chemical studies applying the density-functional-theory (DFT) method in this field have been reported [16], because the DFT method can better consider electron-correlation energies, obviously reduces the computation expenses, and suits the computation of such a kind of complexes in their ground states as singlet state. It is well documented that the lowest-energy transitions of some polypyridineruthenium(II) complexes can be assigned to metal-to-ligand charge transfer (MLCT), and the HOMO–LUMO energy difference between the corresponding complexes obtained from computations with the DFT/B3LYP method is closely correlative to $\Delta E_{1/2}$ ($E_{1/2ox} - E_{1/2red}$) [17]. The DFT calculations for the stacked DNA base-pair model with backbones have also been reported, and it is well established that the energies of the HOMO and the occupied MO near HOMO are rather high and predominantly populated on the base pairs of DNA [18]. We have recently also reported some DFT results on electronic structures and the related properties of the complexes $[Ru(bpy)_2(6,6'\text{-}2R\text{-}dpq)]^{2+}$, $[M(tap)_3]^{2+}$(M = Fe, Ru, Os), and effects of di-F-substitution sites in the main ligand of $[Ru(bpy)_2(dpq)]^{2+}$ (dpq = dipyrido[3,2-*d*:2′,3′-*f*]quinoxaline; tap = 1,4,5,8-tetraazaphenanthrene) [19]. More recently, we have also reported the trends in DNA binding and related behaviors of some complexes $[Ru(bpy)_2L]$ (L = *o*-hpip, *m*-hpip, and *p*-hpip) and $[RuL_2(pmip)]^{2+}$ (L = bpy, phen, and dmp) based on the DFT studies and the frontier-molecular-orbital theory (*o*-, *m*-, and *p*-hpip = 2-(2-hydroxyphenyl)-, 2-(3-hydroxyphenyl)-, and 2-(4-hydroxyphenyl)-imidazo[4,5-*f*][1,10]phenanthroline; dmp = 2,9-dimethyl-1,10-phenanthroline; pmip = 2-(4-methylphenyl)imidazo[4,5-*f*][1,10]phenanthroline) [20]. These direct theoretical efforts on the level of molecular electronic structures of the complexes should be very significant in guiding experimental works.

In this paper, two novel tridentate ruthenium(II) complexes containing an asymmetric aromatic and a polyamine ligand, $[Ru(dipn)(dptp)](ClO_4)_2$ (**1**·2 $ClO_4^-$) and $[Ru(dipn)(pat)](ClO_4)_2$ (**2**·2 $ClO_4^-$) (dipn = *N*-(3-aminopropyl)-propane-1,3-diamine; dptp = 2-(5,6-diphenyl-1,2,4-triazin-3-yl)-1,10-phenanthroline[1]; pat = 9-(1,10-phenanthrolin-2-yl)acenaphtho[1,2-*e*][1,2,4]triazine[1]) were synthesized and characterized. The different DNA-binding behaviors of both ruthenium(II) complexes were studied by spectroscopic methods and viscosity measurements. Theoretical calculations by DFT for the two complexes were also carried out and further applied to explain the obtained experimental observations. The results should be useful for the further understanding of the selectivity and efficiency of DNA recognition by different tridentate ruthenium(II) complexes, as well as for the development of new useful DNA photoprobes and photoreagents.

---

[1]) Formerly, the abbreviations dppt (3-(1,10-phenanthrolin-2-yl)-5,6-diphenyl-*as*-triazine) instead of dptp, and pta (3-(1,10-phenanthrolin-2-yl)-*as*-triazino[5,6-*f*]acenaphthylene) instead of pat were used.

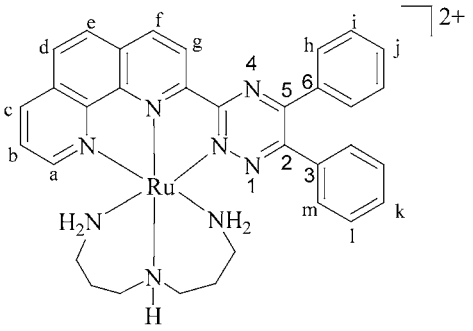

**1** **[Ru(dipn)(dptp)]$^{2+}$**

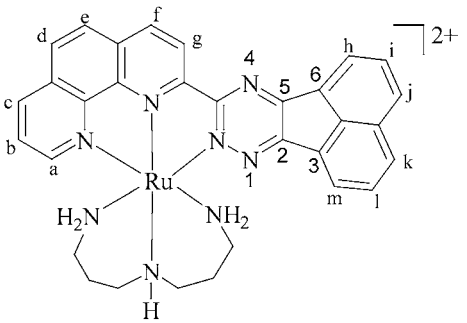

**2** **[Ru(dipn)(pat)]$^{2+}$**

**2. Results and Discussion.** – 2.1. *Synthesis and Characterization*. The complexes **1** and **2** were prepared by direct reaction of the polyamine ligand dipn with the precursor complexes [$RuCl_3$(dptp)] or [$RuCl_3$(pat)], respectively, in the appropriate mol ratios in EtOH/$H_2O$. The yields were good to moderate in each case. The desired ruthenium(II) complexes were isolated as the perchlorates and purified by column chromatography. In the ES-MS for the complexes, only the signals of $[M - ClO_4^-]^+$ and $[M - 2\ ClO_4^-]^{2+}$ were observed. The deduced $M_r$ were consistent with expected values.

All of the new ruthenium(II) complexes gave well-defined $^1$H-NMR spectra (see *Exper. Part*). The $\delta$(H) values were assigned with the aid of $^1$H,$^1$H-COSY experiments and comparison with those of similar compounds [21–25]. A representative $^1$H,$^1$H-COSY plot of [Ru(dipn)(pat)]$^{2+}$ (**2**) is shown in *Fig. 1*. Signals of the protons attached to the phenanthroline moieties appear at lower magnetic fields than those of the free ligands, the downfield shifts of protons in *para*-position to the coordinated N-atom are especially pronounced. Concurrently, the protons close to the metal ion all experience much larger shifts, which is most clearly demonstrated with $H_m$ (0.17 ppm downfield shift for [Ru(dipn)(dptp)]$^{2+}$ (**1**) and 0.65 ppm for [Ru(dipn)(pat)]$^{2+}$ (**2**) in comparison with the corresponding protons of the free ligands). This may be mainly attributed to the electron-withdrawing effects of the metal center, and indirectly to the $\sigma$-donating effect of the tris-amine ligand.

2.2. *Electrochemical Studies*. The electrochemical behavior of the complexes **1** and **2** were studied in MeCN by cyclic voltammetry (CV). Both complexes exhibit well-defined waves corresponding to the metal-based oxidation and successive ligand-based reduction in the sweep range between $-2.0$ and 1.6 V; the half-wave potentials of **1** and **2** and of the homoleptic complexes [$Ru(dptp)_2$]$^{2+}$ and [$Ru(pat)_2$]$^{2+}$ for comparison are listed in *Table 1*; the cyclic voltammograms are given in *Fig. 2*. The anodic- and cathodic-peak separations vary from 61 to 72 mV and are nearly independent of the scan rate, indicating that the processes are reversible and belong to a one-electron transfer.

The half-wave potentials based on metal-center oxidation are observed at 1.06 and 1.18 V for complex **1** and **2**, respectively. The oxidation of **2** shifts the potential to more positive values, suggesting that the pat ligand can better stabilize the $Ru^{II}$ state than dptp, which is consistent with the stronger electron-withdrawing ability of pat. At the

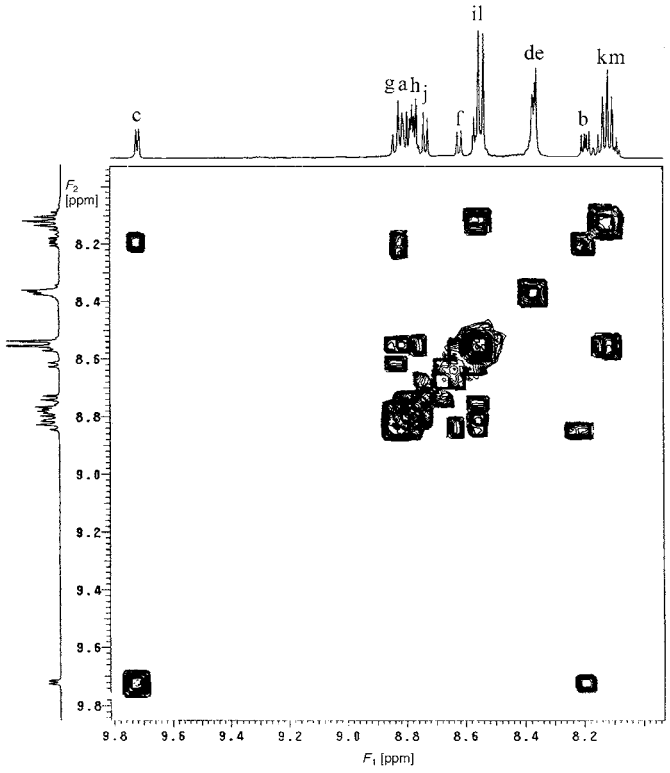


Fig. 1. *$^1H,^1H$-COSY Plot of [Ru(dipn)(pat)]$^{2+}$* (**2**) *in ($D_6$)DMSO* (500 MHz). See *Formula* **2** for atom labels.

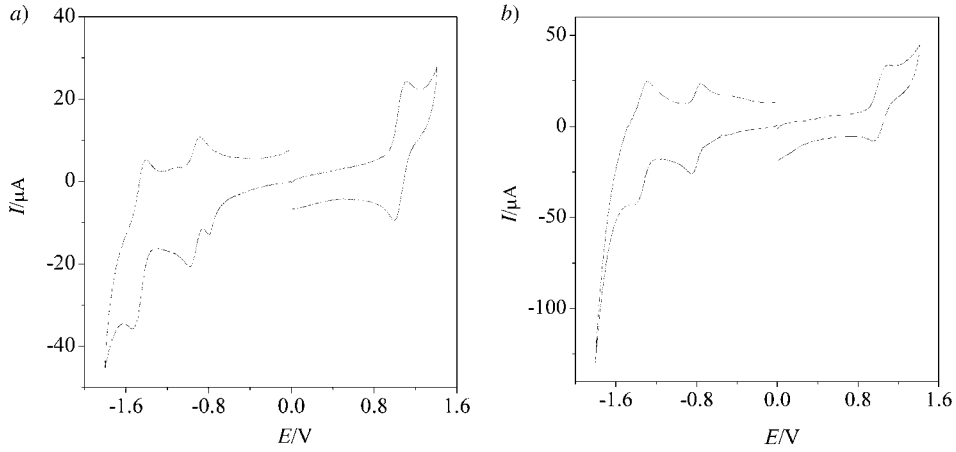


Fig. 2. *Cyclic voltammogram of* a) *[Ru(dipn)(dptp)]$^{2+}$* (**1**) *and* b) *[Ru(dipn)(pat)]$^{2+}$* (**2**) *in MeCN*

Table 1. *Redox Potentials for the Ruthenium(II) Complexes*[a])

| | $Ru^{III}/Ru^{II}$ | Ligand reduction [V] | |
|---|---|---|---|
| | | Potential 1 | Potential 2 |
| $[Ru(dipn)(dptp)]^{2+}$ (**1**) | 1.06 | – 0.93 | – 1.48 |
| $[Ru(dipn)(pat)]^{2+}$ (**2**) | 1.18 | – 0.81 | – 1.37 |
| $[Ru(dptp)_2]^{2+}$ [b]) | 1.35 | – 0.83 | – 1.03 |
| $[Ru(pat)_2]^{2+}$ [b]) | 1.40 | – 0.75 | – 0.95 |

[a]) All complexes were measured in 0.1M $Bu_4NClO_4$/MeCN; error in potentials was $\pm 0.02$ V; $T$ 23 $\pm$ 1°; scan rate 100 mV. [b]) Values from [21].

same time, the oxidation potentials of **1** and **2** are less positive than those of the corresponding compounds $[Ru(dptp)_2]^{2+}$ and $[Ru(pat)_2]^{2+}$ [21]; this can be attributed to the smaller electron-donor capacity of dptp and pat in comparison with that of dipn, thus reducing the electron density at the $Ru^{II}$ center, which hampers the oxidation of $Ru^{II}$ to $Ru^{III}$. By comparison with similar complexes [21][25][26], the reduction potentials of **1** and **2** can be rationally attributed to the ligand-based reductions $L^{0/-1}$ and $L^{-1/-2}$ (L = dptp, pat).

2.3. *Electronic Absorption Spectra*. The absorption spectra of the complexes **1** and **2** in the absence and presence of calf-thymus DNA at various complex concentrations are given in *Fig. 3*. The patterns and shapes of the spectra are similar to those of the structurally corresponding homoleptic complexes $[Ru(dptp)_2]^{2+}$ and $[Ru(pat)_2]^{2+}$ reported previously [21]. The absorption spectra of **1** and **2** are characterized by an intense MLCT transition in the VIS region, and a $\pi-\pi^*$ ligand transition in the UV region; concurrently, the maxima of the MLCT bands of **1** and **2** are significantly shifted to lower energies in comparison with those of $[Ru(dptp)_2]^{2+}$ and $[Ru(pat)_2]^{2+}$. It is well documented in the literature that the energy of the MLCT transitions of $Ru^{II}$ complexes are influenced by the $\pi$-back bonding of ligands [26]. Upon replacing one aromatic ligand with an amine chelate, the back bonding will decrease and the ligand-field splitting will be smaller, thus the MLCT transitions will shift to higher wavelength.

With increasing DNA concentration, the hypochromism increases although no obvious red-shift in the MLCT band of the complexes is observed. When the amount of DNA was increased, the decreases in the MLCT transitions are 8.08% and 25.08% for complexes **1** and **2**, respectively. The hypochromism of **2** is much larger than that of **1**, and even comparable with those of many other so-called intercalative complexes such as $[Ru(bpy)_2(pip)]^{2+}$ [27], $[Ru(bpy)_2(qtpy)]^{2+}$ [28], and $[Ru(phen)_2(phi)]^{2+}$ (pip = 2-phenylimidazo[4,5-*f*][1,10]phenanthroline; qtpy = quaterpyridine; phi = phenanthrene-9,10-diimine) [29].

To compare quantitatively the binding affinity of the complexes **1** and **2**, their intrinsic binding constants to calf-thymus DNA were measured by determining the changes in the absorbance at 536 and 558 nm for **1** and **2**, respectively, with increasing concentration of DNA. *Eqn. 1* was applied [30], where [DNA] is the concentration of DNA in base pairs, and $\varepsilon_a$, $\varepsilon_f$, and $\varepsilon_b$ correspond to the apparent absorption coefficient $A_{obsd}/[Ru]$, the extinction coefficient for the free $Ru^{II}$ complex, and the extinction coefficient for the $Ru^{II}$ complex in the fully bound form, respectively. In plots of $[DNA]/(\varepsilon_a - \varepsilon_f)$ *vs.* [DNA], $K_b$ is given by the ratio of the slope to the intercept.

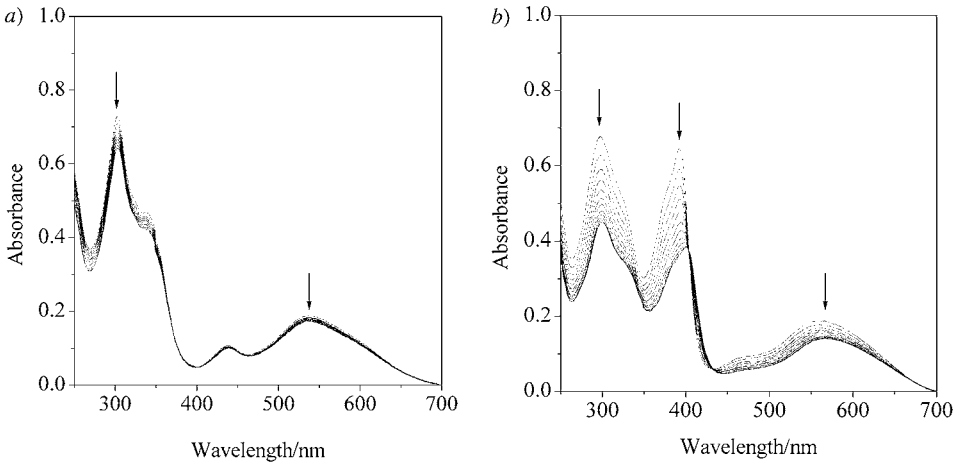


Fig. 3. *Absorption spectra of* a) *[Ru(dipn)(dptp)]*$^{2+}$ (**1**) *and* b) *[Ru(dipn)(pat)]*$^{2+}$ (**2**) *in the presence of increasing amounts of DNA after subtraction of the DNA absorbance.* [Ru] = 20 μM, [DNA] = 0–160 μM. The arrows show the absorbance changes on increasing DNA concentration.

Intrinsic binding constants $K_b$ of $7.61 \cdot 10^3$ M$^{-1}$ and $4.63 \cdot 10^4$ M$^{-1}$ were obtained for **1** and **2**, respectively (*Fig. 4*). These values are comparable to that observed for $[Ru(phen)_2(phi)]^{2+}$ ($2.72 \cdot 10^4$ M$^{-1}$) [29], but smaller than those observed for $[Ru(bpy)_2(dppz)]^{2+}$ ($> 10^6$ M$^{-1}$) [31] and $[Ru(ip)_2(dppz)]^{2+}$ ($2.1 \cdot 10^7$ M$^{-1}$) (dppz = dipyridophenazine; ip = imidazo[4,5-*f*][1,10]phenanthroline) [32]. Considering the planar $\pi$ framework in pat, it is not surprising that complex **2** exhibits better DNA-binding properties than complex **1**. It is also interesting to note that the binding constants of **1** and **2** are slightly smaller than those observed for the related $[Ru(tpy)(dptp)]^{2+}$ and $[Ru(tpy)(pat)]^{2+}$, respectively (tpy = 2,2′:6′,2″-terpyridine) [15a]. This may be due to direct H-bonding between the NH group of the dipn ligand to the O- and N-atoms of bases as well as to neighboring phosphate groups of the DNA, similar to the interactions observed in $[Ru(NH_3)_4(dppz)]^{2+}$ with DNA [33], lowering the binding affinity.

$$[DNA]/(\varepsilon_a - \varepsilon_f) = [DNA]/(\varepsilon_b - \varepsilon_f) + 1/[K_b(\varepsilon_b - \varepsilon_f)] \quad (1)$$

2.4. *Thermal Denaturation Study.* Thermal behaviors of DNA in presence of complexes can give insight into their conformational changes when temperature is raised, and offer information about the interaction strength of complexes with DNA. It is well known that when the temperature in the solution increases, the double-stranded DNA gradually dissociates to single strands, which generates a hyperchromic effect on the absorption spectra of DNA bases ($\lambda_{max}$ 260 nm). To identify this transition process, the melting temperature $T_m$, which is defined as the temperature where half of the total base pairs is unbonded, is usually introduced. According to [34–36], the intercalation of natural or synthetic organics and metallointercalators generally results in a considerable increase in melting temperature ($T_m$). Here, a DNA-melting experiment

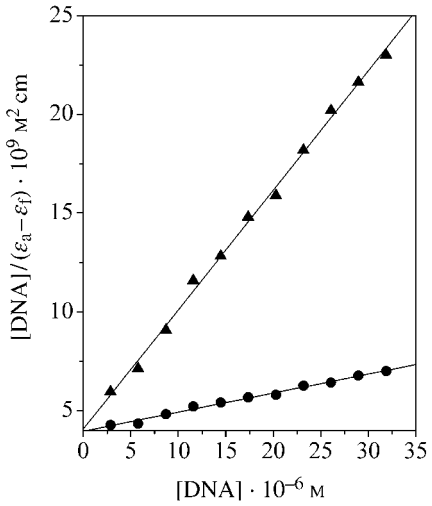


Fig. 4. *Linear-fitting plots of [DNA]/($\varepsilon_a - \varepsilon_f$)* vs. *[DNA] for the absorption titration of DNA with [Ru(dipn)(dptp)]$^{2+}$* (**1**; ●) *and [Ru(dipn)(pat)]$^{2+}$* (**2**; ▲)

revealed that $T_m$ of calf-thymus DNA is $73 \pm 0.2°$ in the absence of the complexes (*Fig. 5*). The $T_m$ of the DNA bound with complex **1** increases to $76 \pm 0.2°$. The $\Delta T_m$ of 3° indicates that the binding of complex **1** to DNA is weak. This is also reflected in the binding constant. In contrast, on addition of complex **2**, the $T_m$ of the DNA increases dramatically to $82 \pm 0.2°$. The large increase ($\Delta T_m \approx 9°$) in $T_m$ of the latter is comparable to that observed for classical intercalators [34–36].

2.5. *Viscosity Studies.* To further elucidate the binding mode of the present complexes, viscosity measurements were carried out on calf-thymus DNA by varying the concentration of the added complexes. In fact, optical photophysical probes generally provide necessary but not sufficient clues to support a binding mode.

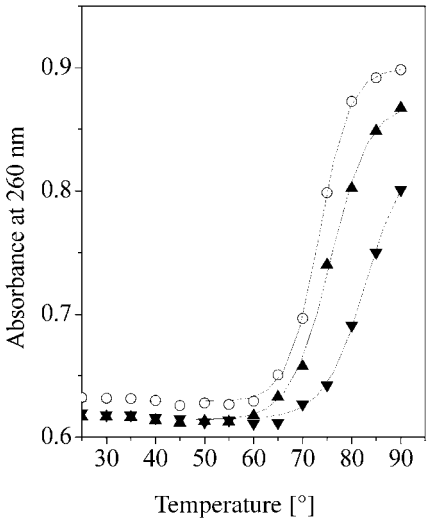


Fig. 5. *Melting curves of DNA in the absence* (○) *and in the presence of complex* **1** (▲) *and complex* **2** (▼)

Viscosity measurements that are sensitive to length change of DNA are regarded as the least ambiguous and the most critical tests of binding mode in solution in the absence of crystallographic structural data or NMR spectra [37][38]. It is popularly accepted that a classical intercalation mode results in lengthening the DNA helix, as base pairs are separated to accommodate the binding ligand, leading to an increase of DNA viscosity. In contrast, a partial and/or nonclassical intercalation of ligand could bend (or kink) the DNA helix, reduce its effective length and, concomitantly, its viscosity [37][38].

The results of viscosity measurements for complexes **1** and **2** are given in *Fig. 6*. The viscosity of DNA decreases upon increasing the concentration of **1**. By contrast, when the amount of **2** is increased, the relative viscosity of DNA increases steadily. These results suggest that the two complexes could bind DNA in two different modes: complex **2** binds to DNA in a classical intercalation mode, whereas complex **1** binds to DNA in a partial intercalation mode. Due to its extended planar ligands, complex **2** can intercalate into DNA base pairs deeply and shows stronger DNA-binding affinity than complex **1**. This is consistent with the spectroscopic results above.

2.6. *Theoretical Explanations of the Trends in DNA Binding, and Electrochemical and Spectral Properties of the Complexes.* The electronic structures of both base pairs of DNA and the intercalative ligand of a metal complex are characteristic of extensive $\pi$-electron delocalization systems. So, the $\pi-\pi$ interaction between the base pairs of DNA and the intercalative ligand of a metal complex in the intercalation mode is rather important. At present, we cannot yet compute a whole supramolecular system formed from DNA and the complex by using the DFT method because such a system is too large in size to be computed. However, the complexes and the DNA model can be individually calculated by the DFT method, and, thus, the trend in the interactions between the complexes and DNA can be analyzed applying the frontier-molecular-orbital theory established by *Fukui* and co-workers [39][40].

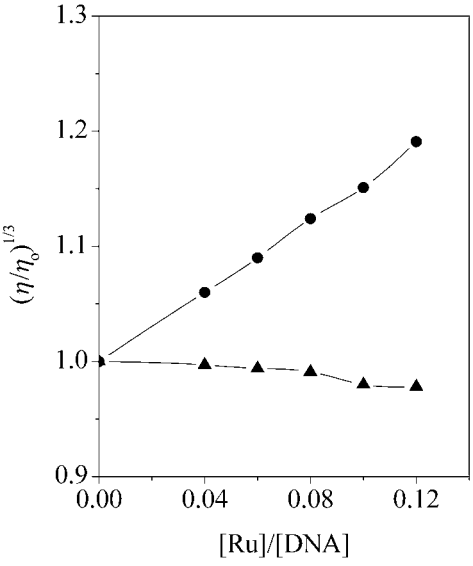


Fig. 6. *Effect of increasing amounts of complex* **1** (▲) *and complex* **2** (●) *on the relative viscosities of DNA at 30.0 ± 0.1°.* [DNA] = 0.5 mM and [Ru]/[DNA] = 0.04, 0.06, 0.08, 0.10, and 0.12.

According to the frontier-molecular-orbital theory, for a reaction controlled by orbital interactions between reactant molecules, a higher HOMO energy of one reactant molecule and a lower LUMO energy of the other one are more advantageous for the reaction between the two molecules because an electron easily moves from the HOMO of a reactant to the LUMO of another reactant. A simple and reasonable calculation model and computed results by the DFT method for stacked DNA base pairs with backbones have been reported by *Kruita et al.* [18]. The reported HOMO and NHOMO energies of the DNA section model are much higher (−1.27 and −2.08 eV) [18] than our calculated LUMO and NLUMO energies (*ca.* −8.1 eV) of the complexes $[Ru(dipn)(dptp)]^{2+}$ (**1**) and $[Ru(dipn)(pat)]^{2+}$ (**2**). We believe that such a trend in the relative energies should be kept in the present DNA system because the attraction of metal-complex cations with high positive charges for electrons in the frontier MOs is much stronger than that of various DNA. Furthermore, the 'electronic cloud' of the HOMO and NHOMO in the DNA model is predominantly populated on the base pairs of DNA, whereas the 'electronic cloud' of the LUMO and NLUMO (if they have accepted electrons) are mainly distributed on the intercalative ligands dptp and pat. Such orbital populations are advantageous to orbital overlap between the HOMO of DNA and the LUMO of the complexes in the intercalative mode, so that we can deduce that the $\pi-\pi$ interaction between the complex and DNA in the intercalation mode should be attributed to the LUMO of the complex with lower energy accepting the electron from the HOMO of DNA populated on the base pairs. Therefore, lower LUMO energy of the complex should be advantageous to the DNA binding of the complex in the intercalation mode. From *Table 2* and *Fig. 7*, we can see that $\varepsilon_L(1) > \varepsilon_L(2)$. On the other hand, the planarity area ($S$) of an intercalative ligand of the metal complex is surely also an important factor because the larger the planarity area ($S$) of the intercalative ligand is, the stronger is the $\pi-\pi$-stacking interaction between the intercalative ligand and base pairs of DNA, and thus the greater is the DNA-binding affinity of the complex. By contrary, nonplanarity of the intercalative ligand will sterically hinder its intercalation. From *Table 3* and *Fig. 8*, we can clearly see that the intercalative ligand dptp of complex **1** is not coplanar, whereas the intercalative ligand pat of complex **2** is coplanar. Therefore, both the LUMO energy and planarity area ($S$) of the intercalative ligand of **2** are more advantageous than those of **1**. Therefore, the DNA-binding constant of **2** is much larger than that of **1**, and their DNA-binding modes are also different.

The trend observed in the electrochemical half-wave potentials of the complexes **1** and **2** can be also further explained applying the energy diagram of the frontier

Table 2. *Some Frontier-Molecular-Orbital Energies* ($\varepsilon_i$/atomic unit) *of* **1** *and* **2** (1 atomic unit = 27.21 eV)

| | Occ[a]) | Occ | Occ | HOMO | LUMO | Vir[b]) | Vir | $\Delta\varepsilon_{L\text{-}H}$[c]) | $\Delta\varepsilon_{L\text{-}NH}$ | $\Delta\bar{\varepsilon}$ |
|---|---|---|---|---|---|---|---|---|---|---|
| $[Ru(dipn)(dptp)]^{2+}$ (**1**) | −0.4144 | −0.4103 | −0.4069 | −0.3973 | −0.2969 | −0.2847 | −0.2757 | 0.1004 | 0.1100 | 0.1052 |
| $[Ru(dipn)(pat)]^{2+}$ (**2**) | −0.4168 | −0.4083 | −0.4036 | −0.4012 | −0.2990 | −0.2829 | −0.2744 | 0.1022 | 0.1046 | 0.1034 |

[a]) Occ: Occupied molecular orbital; HOMO (or H): the highest Occ. [b]) Vir: virtual molecular orbital; LUMO (or L): the lowest Vir. [c]) $\Delta\varepsilon_{L\text{-}H}$: energy difference between LUMO and HOMO; $\Delta\varepsilon_{L\text{-}N}$: energy difference between LUMO and NHOMO (next HOMO); $\Delta\bar{\varepsilon}$: $(\Delta\varepsilon_{L\text{-}H} + \Delta\varepsilon_{L\text{-}NH})/2$.

Table 3. *Selected Calculated Bond Lengths* [nm] *and Bond Angles and Dihedral Angles* [°] *of* **1** *and* **2**. See *Formulae* **1** and **2** for atom labels.

| | Ru–$N_m$ [a]) | N–Ru–$N_m$ | C–C(C–N)$_m$ | Ru–$N_{co}$ [b]) | N–Ru–$N_{co}$ | C–C(C–N)$_{co}$ | Dihedral angle | |
|---|---|---|---|---|---|---|---|---|
| $[Ru(dipn)(dptp)]^{2+}$ (**1**) | 0.2086 | 78.5 | 0.1410 | 0.2191 | 88.1 | 0.1527 | −52.9[c]) | −27.9[d]) |
| $[Ru(dipn)(pat)]^{2+}$ (**2**) | 0.2086 | 79.1 | 0.1411 | 0.2191 | 88.2 | 0.1523 | 0.03[c]) | 0.02[d]) |

[a]) Ru–$N_m$: mean bond length between Ru and the coordinating N-atoms of the main ligand. [b]) Ru–$N_{co}$: mean bond length between Ru and the coordinating N-atoms of the co-ligand. [c]) N(1)–C(2)–C(3)–C(m). [d]) N(4)–C(5)–C(6)–C(h).

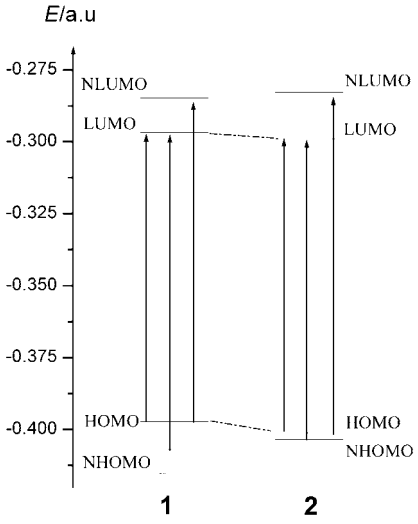


Fig. 7. *Energy diagrams and related* $^1$*MLCT transitions of complex* **1** *and complex* **2**

molecular orbitals (see *Fig. 7*) from the DFT calculations. That the metal-oxidation potential of complex **2** (1.18 V) is shifted to a more positive value as compared to **1** (1.06 V) can be attributed to its HOMO energy being lower than that of complex **1**; the lower HOMO energy implies a more difficult loss of electron from the HOMO. On the other hand, that the ligand-based reduction potential of complex **2** (−0.81 V) is shifted to more positive values as compared to **1** (−0.93 V) can also be rationalized by its LUMO energy being lower than that of complex **1**; the lower LUMO energy implies an easier admission of an electron.

Based on the frontier-molecular-orbital populations on the atoms of the complexes, as shown in *Fig. 8*, we can deduce that the lowest-energy singlet metal-to-ligand-charge-transfer ($^1$MLCT) bands can be assigned to the transitions from the HOMO and NHOMO to the LUMO of the complexes. *Fig. 8* illustrates that the HOMO and NHOMO are characteristic of d-orbitals of the central ions, and the LUMO is characteristic of $\pi$-orbitals of the ligands of the complexes. Furthermore, according to the approximate correlation of the reverse ratio of the difference between the LUMO

and the HOMO energies ($\Delta\varepsilon_{L-H}$) to the experimental wavelength ($\lambda$), by using the parent complex $[Ru(bpy)_3]^{2+}$ as standard ($\lambda_{exper.}$ 452 nm, $\Delta\varepsilon_{L-H} = 0.1239$ a.u. [19a]) and $\Delta\varepsilon_{L-H}$ data of the complexes from *Table 2*, the computed $\lambda_{max}$ values of the $^1$MLCT absorption of the two polypyridineruthenium(II) complexes **1** and **2** are 532 and 542 nm, respectively, near their $\lambda_{exper.}$ values of 536 and 558 nm, respectively.

In addition, the absorption spectra of **1** and **2** also demonstrate that the corresponding energy difference in the presence and absence of DNA is small, and no special pattern changes in the presence of DNA can be detected, except for increases in hypochromism. Therefore, we can consider that there is not a significant effect on the corresponding orbitals of the complexes **1** and **2** on binding to DNA (relative to the free complexes). This further suggests that the interaction between **1** or **2** and DNA should be a weak one so that the property and assignment of the $^1$MLCT bands of **1** and **2** upon binding should be unchanged; this is in accordance with experiments.

**3. Conclusion.** – In summary, two novel ruthenium(II) complexes, $[Ru(dipn)(dptp)](ClO_4)_2$ (**1**·2 $ClO_4^-$) and $[Ru(dipn)(pat)](ClO_4)_2$ (**2**·2 $ClO_4^-$) were synthesized and characterized. The results of spectra titration and viscosity measure-

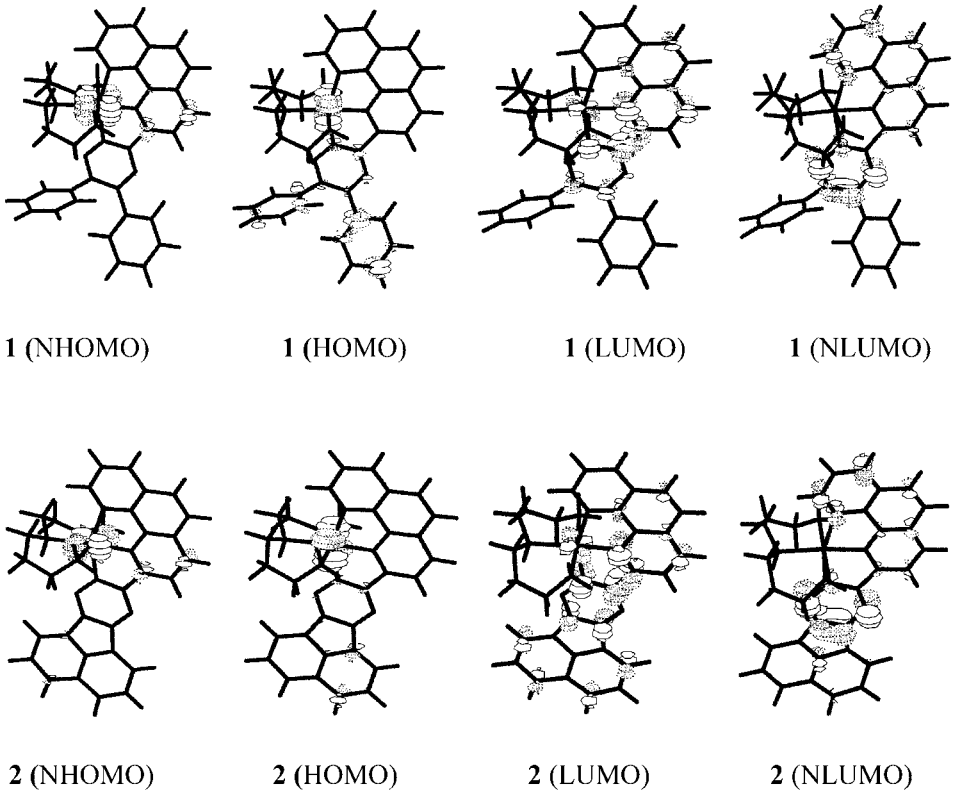


Fig. 8. *Some related frontier molecular orbital stereographs of complex* **1** *and complex* **2**

ments suggest that complex **2** binds to DNA in the classical intercalative mode, and complex **1** binds to DNA in a partially intercalative mode. Theoretical studies for these complexes were also carried out with the density-functional-theory (DFT) method. The trends in the DNA-binding affinity and some electrochemical and spectral properties of the complexes **1** and **2** are further explained applying the DFT-calculation results and the frontier-molecular-orbital theory.

We are grateful to the *National Natural Science Foundation of China*, *National Science Foundation of Guangdong Province*, and *Research Fund of Royal Society of Chemistry U.K.* for their financial supports.

## Experimental Part

*General*. All materials were commercially available and used without further purification unless otherwise noted. Doubly distilled $H_2O$ was used to prepare buffers. Calf-thymus DNA were obtained from the *Sino-American Biotechnology Company*. The ligands dptp and pat were synthesized according to the literature [21][1]). [$RuCl_3$(dptp)] and [$RuCl_3$(pat)] were synthesized similarly as described for [$RuCl_3$(tpy)] [41], by replacing tpy with dptp or pat. *Caution:* perchlorate complexes are potential explosives that must be handled in small quantity and with great care.

Cyclic voltammetry: *EG&G PAR 273* polarographic analyzer and *270* universal programmer; supporting electrolyte, 0.1M ($Bu_4N$)$ClO_4$ in MeCN freshly distilled from $P_2O_5$ and deaerated by purging with $N_2$; standard three-electrode system comprising a Pt microcylinder working electrode, a Pt-wire auxiliary electrode, and a sat.-calomel reference electrode (SCE). UV/VIS Spectra: *Perkin-Elmer-Lambda-35* spectrometers. $^1$H-NMR Spectra: *Varian-Inova-500* spectrometers; $(CD_3)_2SO$ solns. at r.t. and $SiMe_4$ as the internal standard; $\delta$ in ppm, $J$ in Hz. Electrospray-ionization (ESI) MS: *LQC* system (*Finnigan MAT*, USA); MeCN as mobile phase; spray voltage 4.50 KV, tube lens offset 30.00 V, capillary voltage 23.00 V, and capillary temp. 200°; $m/z$ values for the major peaks in the isotope distribution. Microanalyses (C, H, and N): *Perkin-Elmer-240Q* elemental analyzer.

*{N-[3-(Amino-κN)propyl]propane-1,3-diamine-κN,κN′}[2-(5,6-diphenyl-1,2,4-triazin-3-yl-κN$^2$)-1,10-phenanthroline-κN$^1$,κN$^{10}$]ruthenium(2+) Diperchlorate* ([Ru(dipn)(dptp)]$(ClO_4)_2$; **1**·2 $ClO_4^-$). A mixture of [$RuCl_3$(dptp)] (0.14 g, 0.227 mmol), dipn (0.045 g, 0.34 mmol), and $Et_3N$ (1 ml) in EtOH/$H_2O$ 1:1 (*v*/*v*; 50 ml) was refluxed for 8 h (→ purple soln.). After cooling to r.t., the EtOH was evaporated, sat. aq. $NaClO_4$ soln. added, and the purple precipitate purified by column chromatography (neutral alumina, MeCN/EtOH 100:1): 65% of **1**·2 $ClO_4^-$. $^1$H-NMR ($(CD_3)_2SO$; arom. region): 9.70 (*d*, *J* = 5, 1 H); 8.82 (*d*, *J* = 8, 1 H); 8.77 (*d*, *J* = 8.5, 1 H), 8.54 (*dd*, *J* = 3, 3, 1 H); 8.39 (*s*, 2 H); 8.19 (*dd*, *J* = 5, 3, 1 H); 7.77 (*d*, *J* = 7.5, 2 H); 7.73 (*t*, *J* = 5, 1 H); 7.70 (*t*, *J* = 5, 1 H), 7.59–7.53 (*m*, 4 H); 7.50 (*d*, *J* = 7.5, 2 H). ESI-MS (MeCN): 743.1 ([*M* − $ClO_4$]$^+$), 322.3 ([*M* − 2 $ClO_4$]$^{2+}$). Anal. calc. for $C_{33}H_{34}Cl_2N_8O_8Ru$: C 47.11, H 4.07, N 13.25; found: C 47.08, H 4.04, N 13.30.

*{N-[3-(Amino-κN)propyl]propane-1,3-diamine-κN,κN′}[9-(1,10-phenanthrolin-2-yl-κN$^1$,κN$^{10}$)acenaphtho[1,2-e][1,2,4]triazine-κN$^8$]ruthenium(2+) Diperchlorate* ([Ru(dipn)(pat)]$(ClO_4)_2$; **2**·2 $ClO_4^-$). As described for **1**·2 $ClO_4^-$, with [$RuCl_3$(pat)] (0.227 mmol, 0.134 g) instead of [$RuCl_3$(dptp)]: 38% of **2**·2 $ClO_4^-$. Dark purple solid. $^1$H-NMR ($(CD_3)_2SO$; arom. region): 9.72 (*d*, *J* = 5, 1 H); 8.84–8.76 (*m*, 3 H); 8.61 (*d*, *J* = 8, 1 H); 8.57 (*d*, *J* = 8, 1 H); 8.45 (*d*, *J* = 8, 1 H); 8.36 (*dd*, *J* = 5, 3.5, 2 H + 1 H); 8.19 (*dd*, *J* = 5, 3.5, 1 H); 8.13 (*d*, *J* = 8, 1 H); 8.10 (*d*, *J* = 7.5, 1 H). ESI-MS (MeCN): 714.5 ([*M* − $ClO_4$]$^+$), 307.5 ([*M* − 2 $ClO_4$]$^{2+}$). Anal. calc. for $C_{31}H_{30}Cl_2N_8O_8Ru$: C 45.82, H 3.69, N 13.68; found: C 45.80, H 3.68, N 13.74.

*DNA-Binding Experiments*. The spectroscopic titration was carried out in the buffer (5 mM *Tris*·HCl, 50 mM NaCl, pH 7.2) at r.t. For the thermal denaturation study, the buffer containing 15 mM trisodium citrate and 150 mM NaCl (pH 7.0) was used. A soln. of calf-thymus DNA in the buffer gave a ratio of UV absorbance at 260 and 280 nm of *ca.* 1.8–1.9:1, indicating that the DNA was sufficiently free of protein [42]. The DNA concentration per nucleotide was determined by absorption spectroscopy with the molar absorption coefficient (6600M$^{-1}$ cm$^{-1}$) at 260 nm [43]. Stock solns. were stored at 4° and used within 4 days.

The absorption titrations of $Ru^{II}$ complexes in buffer were performed by using a fixed $Ru^{II}$ concentration to which increments of the DNA stock soln. were added. $Ru^{II}$ Solns. employed were 20 μM in concentration, and calf-thymus DNA was added to a ratio [DNA]/[Ru] of 8:1. DNA/Ru solns. were allowed to incubate for 10 min before the absorption spectra were recorded.

Thermal denaturation studies were carried out with a *Perkin-Elmer-Lambda-35* spectrophotometer equipped with a *Peltier* temperature-controlling programmer (±0.1°). The absorbance at 260 nm was

continuously monitored for solns. of calf-thymus DNA (100 μM) in the absence and presence of complex (10 μM). The temp. of the soln. was increased by 1° $min^{-1}$.

Viscosity measurements were performed with an *Ubbelodhe* viscometer maintained at $30.0 \pm 0.1°$ in a thermostatic bath. DNA Samples with an approximate average length of 200 base pairs were prepared by sonication to minimize complexities arising from DNA flexibility [44]. Flow time was measured with a digital stopwatch, and each sample was measured three times, and an average flow time was calculated. Data were presented as $(\eta/\eta^0)^{1/3}$ *vs.* binding ratio ([Ru]/[DNA]) [45], where $\eta$ is the viscosity of DNA in the presence of complex and $\eta^0$ is the viscosity of DNA alone.

*Theoretical Calculations*. Each complex forms from a $Ru^{II}$ ion, one main ligand or intercalative ligand (dptp or pat), and one ancillary ligand (dipn). All computations were performed with the G98 quantum-chemistry program package [46], and the DFT-B3LYP method [47–50] and LanL2DZ basis set [51][52] were adopted. The full geometry-optimization computations for the ground states of these complexes with singlet state were carried out. To vividly depict the details of the frontier-molecular-orbital interactions, the stereographs of some related frontier molecular orbitals of the complexes were drawn with the Molden v3.7 program [53] based on the obtained computational results.

## REFERENCES


[1] D. M. Perrin, A. Mazumder, D. S. Sigman, in 'Progress in Nucleic Acid Chemistry and Molecular Biology', Vol. 52, Eds. W. Cohn and K. Moldave, Academic Press, New York, Orlando, 1996, p. 123.

[2] 'Metal Ions in Biological Systems', Vol. 33, Eds. A. Sigel and H. Sigel, Marcel Dekker, New York, 1996.

[3] G. Pratvicl, J. Bernadou, B. Mcunicr, *Adv. Inorg. Chem*. **1998**, *45*, 251.

[4] K. E. Erkkila, D. T. Odom, J. K. Barton, *Chem. Rev.* **1999**, *99*, 2777.

[5] C. Moucheron, A. K. D. Mesmaerer, J. M. Kelly, in 'Structure and Bonding', Vol. 92, Ed. M. J. Clarke, Springer-Verlag, Berlin, 1998, p. 163.

[6] Y. Xiong, L. N. Ji, *Coord. Chem. Rev.* **1999**, *185–186*, 711; L. N. Ji, X. H. Zou, J. G. Liu, *Coord. Chem. Rev.* **2001**, *216–217*, 513; J.-G. Liu, B.-H. Ye, Q.-L. Zhang, X.-H. Zou, Q.-X. Zhen, X. Tian, L.-N. Ji, *J. Biol. Inorg. Chem.* **2000**, *5*, 119; X.-H. Zou, B.-H. Ye, H. Li, Q.-L. Zhang, H. Chao, J.-G. Liu, L.-N. Ji, *J. Biol. Inorg. Chem*. **2000**, *6*, 143.

[7] I. Ortmans, C. Moucheron, A. Kirsch-De Mesmaeker, *Coord. Chem. Rev.* **1998**, *168*, 233.

[8] A. Ambroise, B. G. Maiya, *Inorg. Chem.* **2000**, *39*, 4256; A. Ambroise, B. G. Maiya, *Inorg. Chem*. **2000**, *39*, 4264.

[9] E. Tuite, P. Lincolin, B. Nordén, *J. Am. Chem. Soc*. **1997**, *119*, 239; B. Önfelt, P. Lincoln, B. Nordén, *J. Am. Chem. Soc.* **1999**, *121*, 10846; L. M. Wilhelmsson, F. Westerlund, P. Lincoln, B. Nordén, *J. Am. Chem. Soc.* **2002**, *124*, 12092.

[10] J. G. Collins, J. R. Aldrich-Wright, I. D. Greguric, P. A. Pellegrini, *Inorg. Chem*. **1999**, *38*, 3502; B. T. Patterson, J. G. Collins, F. M. Foley, F. R. Keene, *J. Chem. Soc., Dalton Trans.* **2002**, 4343.

[11] P. K. L. Fu, P. M. Bradley, D. van Loyen, H. Durr, S. H. Bossmann, C. Turro, *Inorg. Chem.* **2002**, *41*, 3808.

[12] F. O'Reilly, J. Kelly, A. Kirsch-De Mesmaeker, *J. Chem. Soc., Chem. Commun.* **1996**,1013; F. M. O'Reilly, J. M. Kelly, *New J. Chem.* **1998**, 215; F. M. O'Reilly, J. M. Kelly, *J. Phys. Chem. B.* **2000**, 104, 7206.

[13] K. K. Patel, E. A. Plummer, M. Darwish, A. Rodger, M. J. Hannon, *J. Inorg. Biochem.* **2002**, *91*, 220.

[14] V. G. Vaidyanathan, B. U. Nair, *J. Inorg. Biochem.* **2002**, *91*, 405.

[15] a) H. Chao, W. J. Mei, Q. W. Huang, L. N. Ji, *J. Inorg. Biochem.* **2002**, *92*, 165; b) C. W. Jiang, H. Chao, H. Li, L. N. Ji, *J. Inorg. Biochem.* **2003**, *93*, 247.

[16] W. J. Frisch, A. Frisch, J. B. Foresman, 'Gaussian 94 User's Reference', Gaussian Inc.; Pittsburgh, PA, 1994–1995.

[17] S. R. Stoyanov, J. M. Villegas, D. P. Rillema, *Inorg. Chem.* **2002**, *41*, 2941.

[18] N. Kurita, K. Kobayashi, *Comput. Chem.* **2000**, *24*, 351.

[19] a) K. C. Zheng, J. P. Wang, W. L. Peng, X. W. Liu, F. C. Yun, *J. Phys. Chem. A.* **2001**, *105*, 10899; b) K. C. Zheng, J. P. Wang, Y. Shen, W. L. Peng, F. C. Yun, *J. Chem. Soc., Dalton Trans.* **2002**, 111; c) K. C. Zheng, Y. Shen, J. P. Wang, X. W. Liu, F. C. Yun, *Inorg. Chim. Acta* **2002**, *335*, 100.

[20] W. J. Mei, J. Liu, K. C. Zheng, L. J. Lin, H. Chao, A. X. Li, F. C. Yun, L. N. Ji, *J. Chem. Soc., Dalton Trans.* **2003**, 1352; H. Xu, K. C. Zheng, H. Deng, L. J. Lin, Q. L. Zhang, L. N. Ji, *New J. Chem.* **2003**, *27*, 1255.

[21] H. Chao, G. Yang, G. Q. Xue, H. Li, H. Zhang, I. D. Williams, L. N. Ji, X. M. Chen, X. Y. Li, *J. Chem. Soc., Dalton Trans.* **2001**, 1326.

[22] R. R. Ruminski, S. Underwood, K. Vallely, S. J. Smith, *Inorg. Chem.* **1998**, *37*, 6528.

[23] Y. Jahng, R. P. Thummel, S. G. Bott, *Inorg. Chem.* **1997**, *36*, 3133.
[24] E. C. Constable, J. E. Davies, D. Phillips, P. R. Raithby, *Polyhedron* **1998**, *17*, 3989.
[25] G. A. Mines, J. A. Roberts, J. T. Hupp, *Inorg. Chem.* **1992**, *31*, 125.
[26] N. Aydin, C. W. Schlaepfer, *Polyhedron* **2001**, *20*, 37.
[27] J. Z. Wu, B. H. Ye, L. Wang, L. N. Ji, J. Y. Zhou, R. H. Li, Z. Y. Zhou, *J. Chem. Soc., Dalton Trans.* **1997**, 1395.
[28] R. J. Morgan, S. Chatterjee, A. D. Baker, T. C. Strekas, *Inorg. Chem.* **1991**, *30*, 2687.
[29] A. M. Pyle, J. P. Rehmann, R. Meshoyrer, C. V. Kumar, N. J. Turro, J. K. Barton, *J. Am. Chem. Soc.* **1989**, *111*, 3051.
[30] A. Wolf, G. H. Shimer Jr., T. Meehan, *Biochemistry* **1987**, *26*, 6392.
[31] A. E. Friedman, J. C. Chambron, J.-P. Sauvage, N. J. Turro, J. K. Barton, *J. Am. Chem. Soc.* **1990**, *112*, 4960.
[32] J. G. Liu, B. H. Ye, H. Li, L. N. Ji, R. H. Li, J. Y. Zhou, *J. Inorg. Biochem.* **1999**, *73*, 117.
[33] R. B. Nair, E. S. Teng, S. L. Kirkland, C. J. Murphy, *Inorg. Chem.* **1998**, *37*, 139.
[34] M. J. Waring, *J. Mol. Biol.* **1965**, *13*, 269.
[35] J. M. Kelly, A. B. Tossi, D. J. McConell, C. OhUigin, *Nucleic Acids Res.* **1985**, *13*, 6017.
[36] G. A. Neyhart, N. Grover, S. R. Smith, W. A. Kalsbeck, T. A. Fairly, M. Cory, H. H. Thorp, *J. Am. Chem. Soc.* **1993**, *115*, 4423.
[37] S. Satyanarsyana, J. C. Dabroniak, J. B. Chaires, *Biochemistry* **1992**, *31*, 9319.
[38] S. Satyanarsyana, J. C. Dabroniak, J. B. Chaires, *Biochemistry* **1993**, *32*, 2573.
[39] K. Fukui, T. Yonezawa, H. Shingu, *J. Chem. Phys.* **1952**, *20*, 722.
[40] I. Fleming, 'Frontier Orbital and Organic Chemical Reaction', Wiley, New York, 1976.
[41] B. P. Sullivan, J. M. Calvert, T. J. Meyer, *Inorg. Chem.* **1980**, *19*, 1404.
[42] J. Marmur, *J. Mol. Biol.* **1961**, *3*, 208.
[43] M. F. Reichmann, S. A. Rice, C. A. Thomas, P. Doty, *J. Am. Chem. Soc.* **1954**, *76*, 3047.
[44] J. B. Chaires, N. Dattagupta, D. M. Crothers, *Biochemistry* **1982**, *21*, 3933.
[45] G. Cohen, H. Eisenberg, *Biopolymers* **1969**, *8*, 45.
[46] M. J. Frisch, G. W. Trucks, H. B. Schlegel, G. E. Scuseria, M. A. Robb, J. R. Cheeseman, V. G. Zakrzewski, J. A. Montgomery Jr., R. E. Stratmann, J. C. Burant, S. Dapprich, J. M. Millam, A. D. Daniels, K. N. Kudin, M. C. Strain, O. Farkas, J. Tomasi, V. Barone, M. Cossi, R. Cammi, B. Mennucci, C. Pomelli, C. Adamo, S. Clifford, J. Ochterski, G. A. Petersson, P. Y. Ayala, Q. Cui, K. Morokuma, N. Rega, P. Salvador, J. J. Dannenberg, D. K. Malick, A. D. Raghavachairi, J. B. Foresman, J. Cioslowski, J. V. Ortiz, A. G. Baboul, B. B. Stefanov, G. Liu, A. Liashenko, P. Piskorz, I. Komaromi, R. Gomperts, R. L. Martin, D. J. Fox, T. Keith, M. A. Al-Laham, C. Y. Peng, A. Nanayakkara, M. Challacombe, P. M. W. Gill, B. Johnson, W. Chen, M. W. Wong, J. L. Andres, C. Gonzalez, M. Head-Gordon, E. S. Replogle, J. A. Pople, 'Gaussian 98, Revision A 11.4', Gaussian, Inc., Pittsburgh, PA, 2002.
[47] P. Hohenberg, W. Kohn, *Phys. Rev. B* **1964**, *136*, 864.
[48] A. D. Becke, *J. Chem. Phys.* **1993**, *98*, 1372.
[49] A. Gorling, *Phys. Rev. A* **1996**, *54*, 3912.
[50] J. B. Foresman, E. Frisch, 'Exploring Chemistry with Electronic Structure Methods', 2nd edn., Gaussian Inc., Pittsburgh, PA, 1996.
[51] P. J. Hay, W. R. Eadt, *J. Chem. Phys.* **1985**, *82*, 270.
[52] P. J. Hay, W. R. Eadt, *J. Chem. Phys.* **1985**, *82*, 299.
[53] G. Schaftenaar, J. H. Noordik, *J. Comput.-Aided Mol. Des.* **2000**, *14*, 123.

*Received November 17, 2003*